Journal for Geometry and Graphics
Volume 6 (2002), No. 1, 83–98.

Filling Holes with B-spline Surfaces

Márta Szilvási-Nagy

Department of Geometry, Budapest University of Technology and Economics
Egry József út 1, H. 22., H-1111 Budapest XI, Hungary
email: szilvasi@math.bme.hu

Abstract. This paper presents an algorithm for filling holes with polynomial tensor product B-spline surfaces of degree (3,2). The B-spline surface is constructed as a tube shaped surface which is attached to the boundary of the hole at one end and is tied up in a closing point at the other end. The patches around the closing point are degenerate three-sided patches. The unknown control points and shape influencing tangent magnitudes of the B-spline surface are computed from boundary conditions and fairness criteria by minimizing appropriate energy functions.

Key Words: B-spline surfaces, boundary conditions, fairing

MSC 2000: 53A05, 68U05

1. Introduction

When modelling a surface of arbitrary shape with rectangular patches n-sided holes may arise. The filling of such holes is a classical problem in surface modelling. A piecewise bisextic B-spline surface with regular parametrization is constructed in [7]. A survey of other filling methods and a new construction is given in [6]. The geometric data of bicubically blended Coons patches filling the hole are determined there according to an angular tolerance introduced for the change of the surface normals. A blending surface between a point and a closed curve is constructed in [12] for filling an n-sided hole. The surface is generated there by quintic polynomial transition functions. Both papers mention the problem of determining tangent magnitudes so that the resulting surface becomes well shaped. A solution of this problem in [10] is frequently cited in the literature. In the present paper the tangent magnitudes are computed from fairing conditions.

The algorithm to be presented is based on the boundary control of B-spline surfaces and works on the B-spline representation. The n-sided hole is filled by a polynomial tensor product B-spline surface of bidegree (3,2). It is a tube shaped surface fitted at one end on the boundary of the hole to the surrounding patches continuously. The other end of the tube shaped surface is constructed from degenerate three-sided patches having their common singular vertex at a prescribed closing point with a given surface normal. Tangent magnitudes which are necessary for the definition of the control points of the closing patches are computed

ISSN 1433-8157/$ 2.50

from fairing functionals. Fairing functionals expressing or approximating elastic energy or other physical quantities and geometric constraints can be used effectively not only to smooth surfaces ([3]) but also in interactive shape design ([8]).

The algorithm for filling a hole is structured as follows.

- Construction of a preliminary ring shaped B-spline surface stripe of degree (3,2) such that it fits the boundary curve of the hole and a tangent vector field along it with second order contact. This surface stripe consists of one row (layer) of patches whose control points are determined from the boundary conditions. The parameter lines are cubic in the radial and quadratic in the circular direction.
- Extension of the ring surface into a tube shaped surface towards the center of the hole by two new rows of patches, where the second row consists of degenerate triangular patches with a common singular vertex. The control points of the extension are determined from the closing boundary conditions, which are the closing point and a tangent plane at this point, and froma fairness criterion. In this way the extension will fill up the hole.
- Removing the preliminary surface stripe whose role was to transfer boundary conditions computed from the surrounding surfaces.
- Resmoothing the filling surface with a fairing condition according to prescribed normal curvature values at the closing point.

New points in the algorithm are as follows. The filling algorithm is implemented for B-spline representation therefore, it does not require patchwise adjustment of control points in order to get continuous resulting surface, and no conversion is necessary (compare with [6]). The location of the closing (central) point and magnitudes of the tangent vectors (a central problem in former papers) are computed from a fairness criterion which results a nice, tight shape automatically. Due to quadratic (planar) parameter lines in the circular directions the surface does not wiggle around the closing point between two radial boundary lines of its patches. Nothing has been assumed about the mathematical representation of the surrounding surfaces, only that the second derivatives with exception of a finite number of points exist. The G^1 connection between the filling surface and the surrounding surfaces is as precise, as the second order approximation of the boundary of the hole and the tangent vector field along it. Also a solution is given with prescribed normal curvatures at the closing point.

2. Mathematical description and boundary control

The mathematical description of the tube shaped surface to be constructed is as follows. Let V_{ij}; $i = 0, \ldots, n$; $j = 0, \ldots, m$ be a set of control points, furthermore $B_i^{(3)}(u)$ and $B_j^{(2)}(v)$ be cubic and quadratic B-spline functions defined over the periodic knot vectors of real values $\{t_l\}_{-2}^{n+3}$ and $\{s_k\}_{-1}^{m+2}$, respectively. Then each patch of the B-spline surface is represented by the two-parameter vector-valued function written in matrix form

$$\begin{gathered}\mathbf{r}_{lk}(u,v) = [\,1 \quad u \quad u^2 \quad u^3\,]\,\mathbf{B}_l^{(3)}(t)\mathbf{G}_{lk}[\mathbf{B}_k^{(2)}(s)]^T\,[\,1 \quad v \quad v^2\,]^T , \\ l = 1, \ldots, n-2, \quad k = 1, \ldots, m-1, \quad (u,v) \in [0,1] \times [0,1],\end{gathered} \tag{1}$$

where

$$u = \frac{t - t_{l+2}}{t_{l+3} - t_{l+2}}, \quad v = \frac{s - s_{k+1}}{s_{k+2} - s_{k+1}}$$

are the parameters of the patch. The matrices $\mathbf{B}_l^{(3)}(t)$ and $\mathbf{B}_k^{(2)}(s)$ are the coefficient matrices of the cubic and quadratic basis functions, respectively. In the nonuniform case the matrix elements are expressed by the knot values ([1, 2]), in the uniform case they are constant:

$$\mathbf{B}_l^{(3)}(t) = \mathbf{B}^{(3)} = \frac{1}{6}\begin{bmatrix} 1 & 4 & 1 & 0 \\ -3 & 0 & 3 & 0 \\ 3 & -6 & 3 & 0 \\ -1 & 3 & -3 & 1 \end{bmatrix}, \qquad \mathbf{B}_k^{(2)}(s) = \mathbf{B}^{(2)} = \frac{1}{2}\begin{bmatrix} 1 & 1 & 0 \\ -2 & 2 & 0 \\ 1 & -2 & 1 \end{bmatrix}$$

The geometric data of the (l, k)th patch are included in the matrix $\mathbf{G}_{lk}$. The entries of the matrix

$$\mathbf{G}_{lk} = \begin{bmatrix} V_{l-1,k-1} & V_{l-1,k} & V_{l-1,k+1} \\ V_{l,k-1} & V_{l,k} & V_{l,k+1} \\ V_{l+1,k-1} & V_{l+1,k} & V_{l+1,k+1} \\ V_{l+2,k-1} & V_{l+2,k} & V_{l+2,k+1} \end{bmatrix}$$

are the control points of the (l, k)-th patch $(l = 1, \ldots, n-2,\ k = 1, \ldots, m-1.)$

By assumption, the quadratic v parameter lines are closed cross-sectional curves of the tube, therefore $V_{i,m-1} = V_{i,0}$ and $V_{i,m} = V_{i,1}$, $i = 0, \ldots, n$ must hold. Degree 2 of the v-lines allows second degree approximation of piecewise differentiable surface curves around the hole using their Taylor polynomials of degree 2 or approximating them by quadratic Bézier segments. The longitudinal u parameter lines are cubic curves over the periodic knot vector $t_{-2} < t_{-1} < \ldots < t_{n+3}$ which allows to prescribe boundary conditions, e.g., the end point and either a tangent vector or the curvature at this end point ([11], Chap. 5). Control points determined by boundary conditions are called *phantom points* or *pseudo vertices*. This technique of phantom points has been extended to tensor product B-spline surfaces in ([13, 15]). Another type of phantom points called *quasi control points* have been determined from the condition of cyclical smooth joining of degenerate bicubic Bézier patches around an extraordinary point in [9].

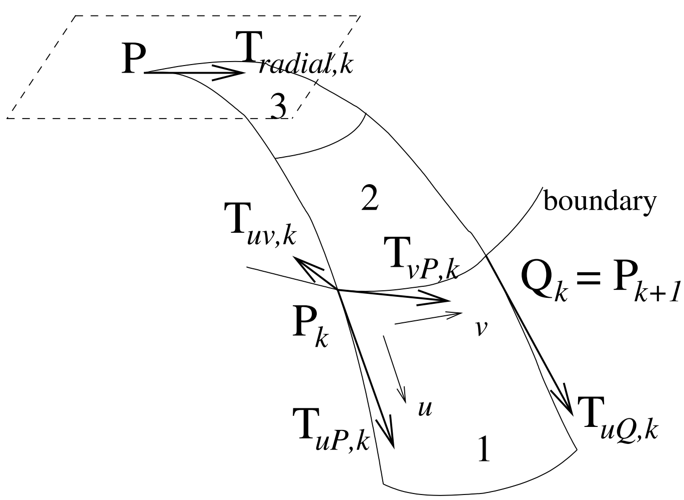

Figure 1: Boundary conditions

Let us assume that first order boundary conditions are given for the bordering patches $(l = 1)$ of the surface given in (1). These are corner points and derivatives at those points (Fig. 1):

$$\mathbf{P}_k \quad = \quad \mathbf{r}_{1k}(0, 0), \tag{2}$$

$$\mathbf{T}_{uP,k} = \frac{\partial}{\partial u}\mathbf{r}_{1k}(0,0), \tag{3}$$

$$\mathbf{T}_{v,k} = \frac{\partial}{\partial v}\mathbf{r}_{1k}(0,0), \tag{4}$$

$$\mathbf{T}_{uv,k} = \frac{\partial^2}{\partial u \partial v}\mathbf{r}_{1k}(0,0), \tag{5}$$

$$\mathbf{Q}_{k} = \mathbf{r}_{1k}(0,1), \tag{6}$$

$$\mathbf{T}_{uQ,k} = \frac{\partial}{\partial u}\mathbf{r}_{1k}(0,1), \quad k = 1,\dots,m-1. \tag{7}$$

How first order boundary conditions determine control points is expressed in the following theorem quoted from [14].

Theorem 1 *Let* $V_{ij}^{(k)}$ $i = 0,\dots,3$, $j = 0,1,2$ *be the control points of a boundary patch* $\mathbf{r}_{1k}(u,v)$ *of the tube shaped tensor product B-spline surface of bidegree (3,2) given by equation (1),* $l = 1$, $1 \le k \le m-1$. *Then the vector equations (2)–(7) determine the control points* $V_{0j}^{(k)}$ *and* $V_{1j}^{(k)}$, $j = 0,1,2$.

In the proof of the theorem the prescribed corner points and the derivatives are expressed from equation (1). These vector equations are linear functions of the control vertices $V_{ij}^{(k)}$, $i = 0,1,2$; $j = 0,1,2$. Keeping the control points in the third row ($i = 2$) fixed, the system of linear vector equations can be solved for the six control points standing in the first two rows of the control net.

Remark: In the case when, in addition to conditions (2)–(7), also the normal curvature value of the parameter line $\mathbf{r}_{1k}(u,0)$ is prescribed at the corner point $u = 0$, a solution has been given in [15] by minimizing a fairness functional under the curvature condition.

3. Construction of a ring shaped stripe around the hole

A preliminary closed stripe represented as a tube shaped B-spline surface given in (1) will be laid around the hole so that it fits the border line of the surrounding surfaces and a tangent vector field along it with contact of second order. That means that the boundary lines of the stripe and that of the hole coincide up to second order, moreover the tangent planes of the two surfaces at the points of the “common” boundary line approximately coincide as well. In the special case of quadratic surrounding surfaces the boundary line and the tangent planes of the constructed B-spline stripe may coincide exactly with those of the surrounding surfaces. The stripe consists of one row (layer) of patches, and it will be extended by two additional rows in order to fill the hole. The preliminary layer transfers the first order boundary conditions from the surrounding surfaces, and after the extension it will be removed. Fig. 6 shows this ring shaped stripe on cylindrical surfaces.

By assumption, the boundary line is composed of curve segments represented by one-parameter twice differentiable vector functions. Similarly, a one-parameter field of vectors pointing in reversed “radial directions” from the center of the hole and being tangential to the surrounding surfaces is also prescribed along the boundary line of the hole, and is represented piecewise by one-parameter twice differentiable vector functions. This tangent field will ensure the G^1 fitting of the B-spline surface to be constructed. The boundary line of the hole and also the tangent field along it have to be split into segments according to the number of the patches of the B-spline. Then each segment has to be represented

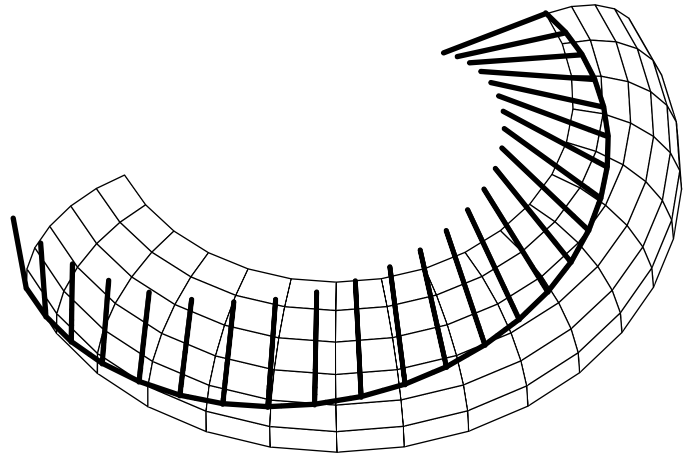

Figure 2: Bézier approximation of a surface curve and tangent field in 6 segments

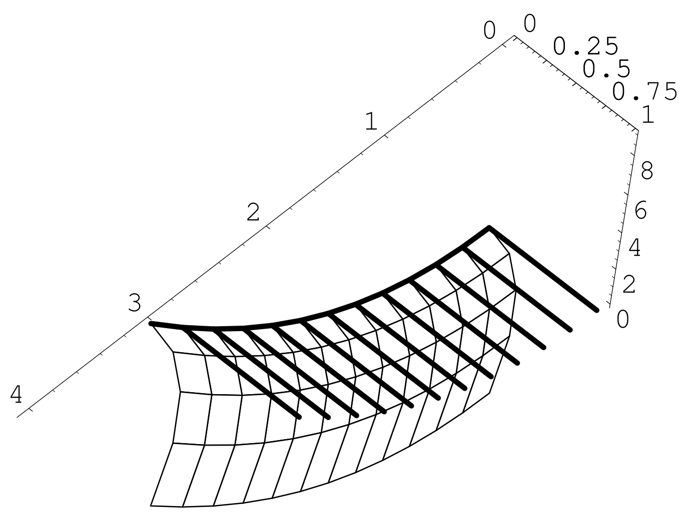

Figure 3: Quadratic surface and tangent field in 3 segments

by a quadratic polynomial vector function of one parameter. This can be done either with quadratic Bézier segments using a standard spline construction method ([5], Chap. 4.4) and choosing appropriate parametrization ([5], Chap. 2.5), or by Taylor polynomials of degree 2. Fig. 2 shows a surface curve on a torus approximated by six quadratic Bézier segments and a tangent vector field along it. In the case when the surfaces surrounding the hole are quadratic in the parameters, therefore also the boundary curve of the hole is described by quadratic functions, only a segmentation of the boundary curve and the tangent field is necessary. (In Fig. 3 a quadratic surface and the input tangent vector field are shown.) Then as many patches will be generated around the hole as many segments are computed.

Let $\mathbf{c}_k(v)$ denote the segments of the boundary curve of the hole and $\mathbf{d}_k(v)$ the tangent field along it ($k = 1, \ldots, m-1$, $v \in [0,1]$), both of them are quadratic functions of v. By assumption, the boundary line $u = 0$ of the kth patch $\mathbf{r}_{1k}(u,v)$ given in (1) and the u-derivatives of the patch along this boundary are equal to $\mathbf{c}_k(v)$ and $\mathbf{d}_k(v)$, respectively. For a single patch of the unknown B-spline stripe the following identities are required:

$$\mathbf{c}_k(v) \equiv \mathbf{r}_{1,k}(0,v) \tag{8}$$

and

$$\mathbf{d}_k(v) \equiv \frac{\partial}{\partial u}\mathbf{r}_{1,k}(0,v), \qquad v \in [0,1]. \tag{9}$$

On the left-hand side the polynomials are given input data, on the right-hand side the coefficients of the polynomials are expressed by the unknown control points of the patch. The vector equations (8) and (9) have three vector coefficients of the polynomials on both sides.

$$\mathbf{a2}_k v^2 + \mathbf{a1}_k v + \mathbf{a0}_k \equiv \mathbf{a2}_B(\mathbf{G}_{1,k})v^2 + \mathbf{a1}_B(\mathbf{G}_{1k})v + \mathbf{a0}_B(\mathbf{G}_{1k}), \tag{10}$$
$$\mathbf{b2}_k v^2 + \mathbf{b1}_k v + \mathbf{b0}_k \equiv \mathbf{b2}_B(\mathbf{G}_{1k})v^2 + \mathbf{b1}_B(\mathbf{G}_{1k})v + \mathbf{b0}_B(\mathbf{G}_{1k}), \quad v \in [0,1], \tag{11}$$

where

$$\mathbf{G}_{1k} = \{V_{i,j}^{(k)}\}_{i=0,1,2;\, j=0,1,2}, \quad k = 1,\ldots,m-1$$

are the vertices of the kth boundary patch. The vertices in the fourth row ($i = 3$) of the control net do not occur, therefore they are prescribed arbitrarily. Moreover, the vertices in the third row ($i = 2$) will be considered as constant input data. The identities (10) and (11) are satisfied if the corresponding coefficients are equal, which yield 6 linear vector equations for 6 unknown control points $V_{0,j}^{(k)}$ and $V_{1,j}^{(k)}$ ($j = 0,1,2$) of the kth patch. Instead of collecting all the $6*(m-1)$ vector equations for the whole stripe in a huge system of equations, a marshing procedure is developed for the computation of control points of the stripe.

Let us start with a proper initial stripe with temporary vertices having the same topological structure as the required stripe as follows. The temporary vertices V_{0k} in the first row of the control net are equal to the start points $\mathbf{P}_k$ of the curve segments ($k = 1,\ldots,m-1$) of the prescribed boundary curve. From now on the control points of the stripe are indexed globally, i.e. $V_{0k} = V_{00}^{(k)}$. Let $\mathbf{T}_{uP,k} \equiv \mathbf{d}_k(0)$ denote the element of the "radial" vector field at the point $\mathbf{P}_k$ computed as directional derivative of the surrounding surface. Then the vertices in the lth row of the control net of the stripe are $V_{l,k} = V_{0k} + \alpha*(l-1)\mathbf{T}_{uP,k}$ ($l = 1,2,3$), where α is an appropriate real number (in the examples 1). For a closed stripe $V_{l0} = V_{l,m-1}$ and $V_{lm} = V_{l1}$ ($l = 0,\ldots,3$) must hold. The knot vectors in both parameter directions are periodic. In the cross-sectional v direction chord-length parametrization, in the "radial" u direction uniform parametrization is appropriate. In this way the temporary B-spline stripe consisting of one layer is generated by the vector equation (1). Then six control vertices of the kth patch ($k = 1,\ldots,m-1$) are recomputed from the G^1 fitting conditions expressed by (10) and (11). While going around the boundary of the hole, the sliding nets of the patches overlap: $V_{i,1}^{(k)} = V_{i,0}^{(k+1)}$ and $V_{i,2}^{(k)} = V_{i,1}^{(k+1)}$, ($i = 0,\ldots,3$). In each step (i.e., for each k) 4 control points influencing the previous $(k-1)$th patch are recomputed. The B-spline surface generated from the control points computed in this way approximates the input boundary curve segments and the tangent vector fields.

Several examples have shown that the approximation is fairly precise. A B-spline surface fitted on the torus along a surface curve with a tangent vector field (Fig. 2) is shown in Fig. 5. The error computed as the integral of the squared difference between the input and the calculated curve segments is decreasing fast when we increase the number of segments. In the case of 6 segments over a quarter of the torus the error was 0.1%, whereas it was 0.01% when computing with 12 segments.

In the special case when the input data are computed from a quadratic surface, the boundary curve is a parameter line of the surface and the tangent vector field is a set of cross-derivatives. If the number of segments is relatively small, a global fitting method on the whole stripe usually works, and the resulting B-spline stripe fits the input data exactly (Fig. 4). The computations with quadratic surfaces ended with a unique solution in the tested examples. However, a generic discussion of the system of equations cannot be given independently of the input data.

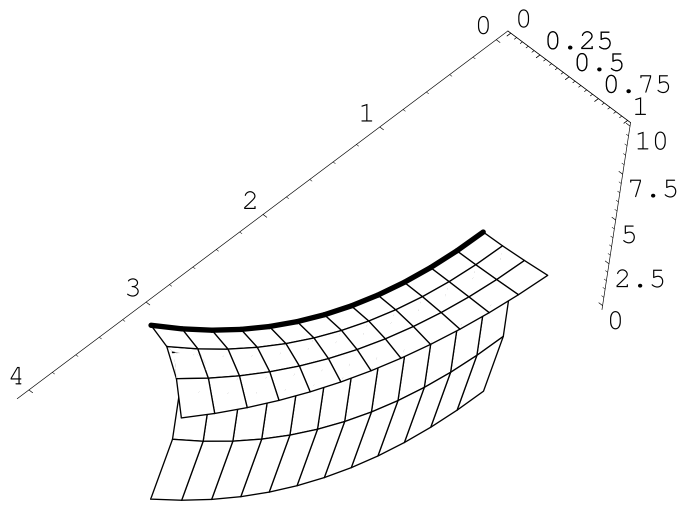

Figure 4: B-spline stripe matching exactly the input data in Fig. 3

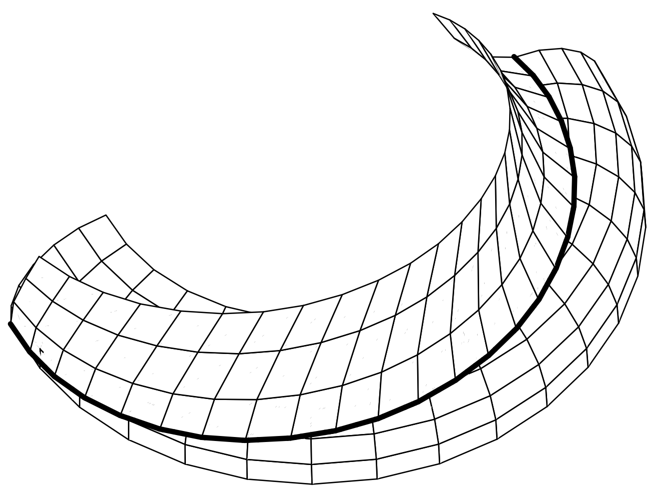

Figure 5: B-spline stripe approximating the input data in Fig. 2

In the examples given for filling a hole the surrounding surfaces are cylindrical patches, the boundary lines of which are quadratic periodic B-spline curves. Therefore, the construction of the control net of the tube shaped stripe laid around the hole has been made directly by glueing the control nets of the cylinders in the cross-sectional direction. In these examples the knot vector in the cross-sectional direction is uniform. The corner points are associated to double control points. A five-sided hole and the B-spline stripe laid around it is shown in Fig. 6. The control net of the stripe to be extended is shown in Fig. 7.

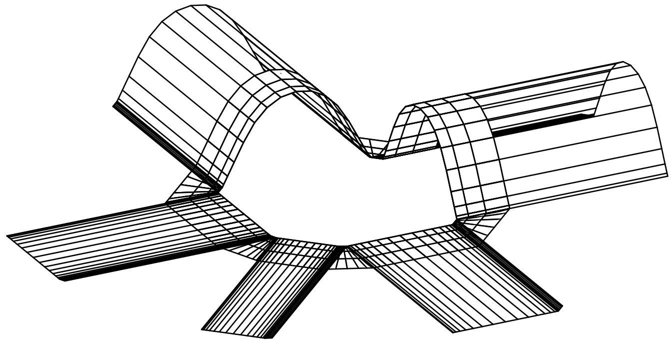

Figure 6: Five-sided hole and the B-spline stripe

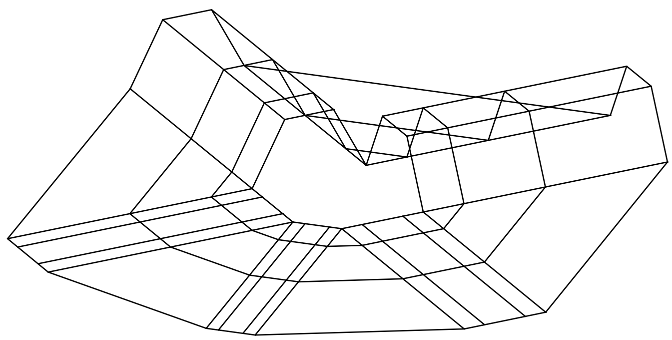

Figure 7: The control net of the stripe

4. Construction of the closing part

Two new rows of patches will be constructed by extending the ring shaped stripe into a tube shaped B-spline surface towards the center of the hole. The vertices V_{ij}, $i = 0, \ldots, 3$; $j = 0, \ldots, m$ of the control net will be renumerated to $i = 2, \ldots, 5$, $j = 0, \ldots, m$, and two rows of phantom control points $V_{0,j}$ and V_{1j}, $j = 0, \ldots, m$ will be computed from first order boundary conditions prescribed at a closing point.

For determining a suitable closing (central) point in the hole and a tangent plane at this point several methods have beeen offered in the literature. In our examples cylindrical surfaces are placed around the vertex of a parallelepiped, therefore the normal of the tangent plane is parallel to the diagonal of the parallelepiped and the closing point is near to the vertex. Both data are user inputs. However, the position of the closing point will be modified by a fairness criterion later on.

Let $\mathbf{P}$ denote the closing point and $\mathbf{N}$ the unit vector of the surface normal at $\mathbf{P}$.

The unknown control points of the extension will be computed from first order boundary conditions (2)–(7) prescribed at $\mathbf{P}$. We require that the cross-sectional quadratic v parameter boundary curves of the bordering patches $\mathbf{r}_{1k}(u, v)$, $k = 1, \ldots, m-1$ shrink to the point $\mathbf{P}$ at $u = 0$. As a consequence, the patches around the closing point are degenerate three-sided patches. The tangent $\mathbf{T}_{radial,\,k}$ of the u parameter line at $v = 0$ of the three-sided patch $\mathbf{r}_{1k}(u, v)$ at the closing point $\mathbf{P}$ is determined from the "radial" directional derivative $\mathbf{T}_{uP,k}$ of the stripe at the corresponding interpolation point of the boundary of the hole by projecting it orthogonally onto the prescribed tangent plane at $\mathbf{P}$ (Fig. 1). However, the degenerate closing patches have no surface normal at their common singular point $\mathbf{P}$, the "radial" u

parameter lines will end up there with a tangent vector lying in the given plane. In this sense the closing patches, regarded as a point set, have a common tangent plane at $\mathbf{P}$. In the cross (circular) direction these patches do not wiggle due to quadratic (planar) v-parameter lines.

The boundary conditions at the center point are the following:

$$\begin{aligned}
\mathbf{P} &= \mathbf{r}_{1k}(0,0), && (12)\\
\lambda_k \mathbf{T}_k^0 &= \frac{\partial}{\partial u}\mathbf{r}_{1k}(0,0), && (13)\\
\mathbf{0} &= \frac{\partial}{\partial v}\mathbf{r}_{1k}(0,0), && (14)\\
\mathbf{0} &= \frac{\partial^2}{\partial u \partial v}\mathbf{r}_{1k}(0,0), && (15)\\
\mathbf{P} &= \mathbf{r}_{1k}(0,1), && (16)\\
\lambda_{k+2} \mathbf{T}_{k+2}^0 &= \frac{\partial}{\partial u}\mathbf{r}_{1k}(0,1), \quad k = 1,\dots,m-2, && (17)
\end{aligned}$$

where $\mathbf{T}_k^0$ in (13) and $\mathbf{T}_{k+2}^0$ in (17) denote the unit vectors of $\mathbf{T}_{radial,\,k}$ and $\mathbf{T}_{radial,\,k+2}$, respectively, lying in the prescribed tangent plane at $\mathbf{P}$. These are the tangent vectors of the kth and $(k+2)$th "radial" patch boundaries at $\mathbf{P}$ and λ_k and λ_{k+2} are there magnitudes, respectively ([14]). The vector magnitudes depending on the parametrization and influencing the shape of the surface are very inconvenient input data. Therefore, they are considered as scalar variables and will be determined from fairness criteria. The equations (14)–(16) are expressing that two corner points of the patch coincide. Consequently, the border line $u = 0$ has zero length and zero tangent vector, also the twist vector is the null vector.

The vector equations (12)–(17) are linear in the control points. The fourth row of the control net does not occur. The control points in the third row are kept fixed, and the control points V_{0j}, V_{1j}, $j = 0,\dots,m$ standing in the first two rows of the control net are the unknowns in the equations.

Let $V_{ij}^{(k)}$, $i = 0,\dots,3$, $j = 0,1,2$, denote the control points of a single bordering patch $\mathbf{r}_{1k}(u,v)$, $1 \le k \le m-2$, $(u,v) \in [0,1]\times[0,1]$, then in the special case of uniform knot vectors the system of equations (12)–(17) has the following solution:

$$\begin{aligned}
V_{00}^{(k)} &= V_{20}^{(k)} - 2\lambda_k \mathbf{T}_k^0, && (18)\\
V_{01}^{(k)} &= V_{21}^{(k)} - 2\lambda_k \mathbf{T}_k^0, && (19)\\
V_{02}^{(k)} &= V_{22}^{(k)} + 2\lambda_k \mathbf{T}_k^0 - 4\lambda_{k+2}\mathbf{T}_{k+2}^0, && (20)\\
V_{10}^{(k)} &= (6\mathbf{P} - 2V_{20}^{(k)} + 2\lambda_k \mathbf{T}_k^0)/4, && (21)\\
V_{11}^{(k)} &= (6\mathbf{P} - 2V_{21}^{(k)} + 2\lambda_k \mathbf{T}_k^0)/4, && (22)\\
V_{12}^{(k)} &= (6\mathbf{P} - 2V_{22}^{(k)} - 2\lambda_k \mathbf{T}_k^0 + 4\lambda_{k+2}\mathbf{T}_{k+2}^0)/4, \quad k = 1,\dots m-2. && (23)
\end{aligned}$$

In the nonuniform case the scalar coefficients are expressed by the parameter intervals of the knot vectors, otherwise the structure of the equations is the same as in the uniform case.

Assuming that all the boundary data in equations (12)–(17) are given by user inputs, the control vertices V_{0j}, V_{1j}, $j = 0,\dots,m$ can be determined successively by moving in the cross-direction $k = 1,\dots,m-2$ on the stripe and storing the solutions (18)–(23) into the control net. Then for closing the surface in the cross-direction $V_{i,m-1} = V_{i0}$ and $V_{im} = V_{i1}$, $i = 0,1$ must hold. Surfaces generated in this way are shown in Figs. 8, 9, 10 and 13.

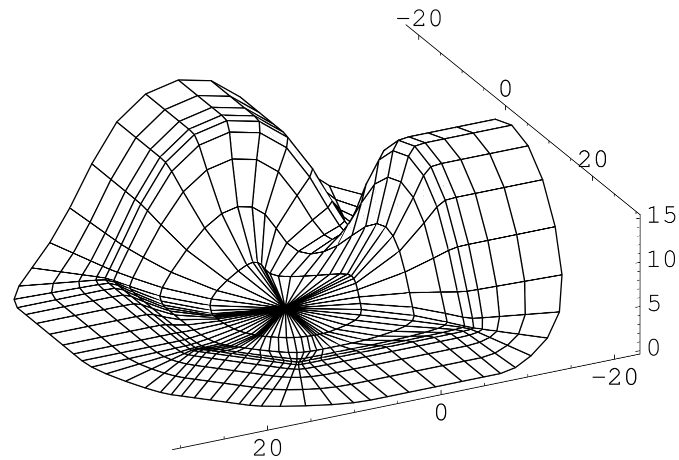

Figure 8: Closing part generated with user specified tangent magnitudes

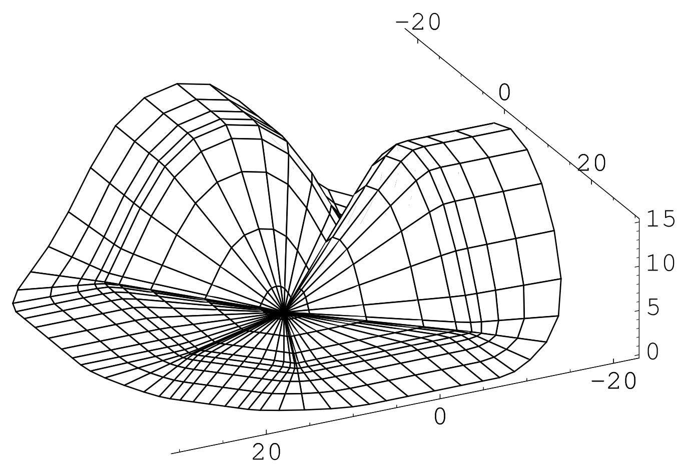

Figure 9: Closing part with zero tangents at the center point

In Figs. 8 and 9 the stripe of Fig. 6 has been extended according to the same user specified closing point, solely the magnitudes of the "radial" tangent vectors at the closing point are

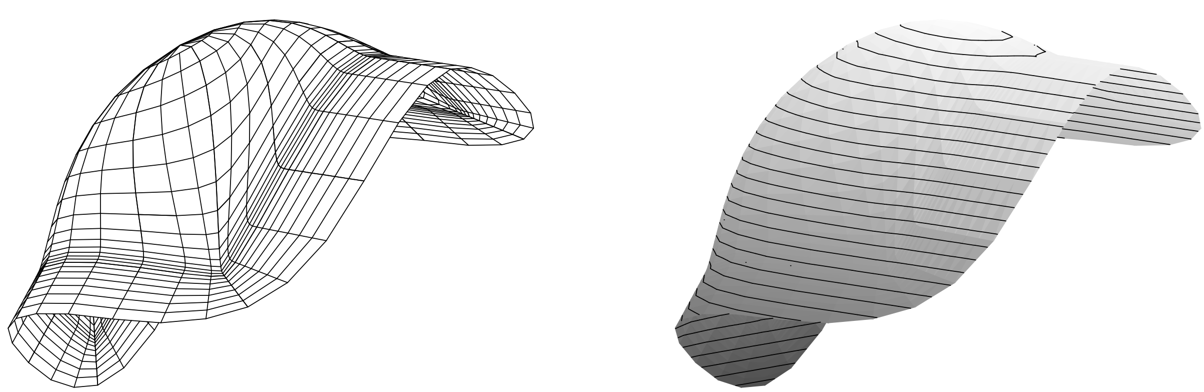

Figure 10: Suitcase corner with user specified closing point and tangent magnitudes

different. In Fig. 8 these magnitudes are 30, obviously too great, when the diameter of the hole is about 32. In Fig. 9 these magnitudes are zero, what leads to a cone shaped closing part. Results of similar computations are shown in Fig. 10 for filling a three-sided hole at a vertex of a cube. The tangent magnitudes at the closing point are 6, while the diameter of the hole is approximately 12. The pictures show the smooth neighbourhood of the singular point due to the fixed tangent plane and quadratic cross sectional parameter lines.

The two rows of patches filling the hole together with the stripe form a surface which is C^2 in the "radial" direction and C^1 in the cross-direction. As the stripe approximates the border line of the hole (or it fits accurately in the quadratic case), and the "radial" tangents are computed from the surrounding surfaces, the filling part joins to the surrounding surfaces with G^1 continuity.

In the case of the shown pentagonal hole the number of bordering patches is 20, in the triagonal case 12, which is too few for reasonable applications, but makes the effect of the data clearer.

5. Fairing conditions

The undesired shaping effect of the user inputs in specifying the closing point and the "radial" tangent magnitudes at the closing point will be eliminated by using fairing conditions. Several examples have been tested, and some are shown in the figures. The applied fairness functionals are quadratic in the partial derivatives of the B-spline vector function, and represent the simplified thin plate energy ([3]), the stiffness matrix ([8]) and a third order energy. These are, respectively,

$$F1(\lambda_1,\dots,\lambda_{m-1}) = \sum_{i,k}\iint_A (\mathbf{r}_{uu}^2 + 2\mathbf{r}_{uv}^2 + \mathbf{r}_{vv}^2)\,dudv \tag{24}$$

$$F2(\lambda_1,\dots,\lambda_{m-1}) = \sum_{i,k}\iint_A (\mathbf{r}_{u}^2 + \mathbf{r}_{v}^2 + \mathbf{r}_{uu}^2 + 2\mathbf{r}_{uv}^2 + \mathbf{r}_{vv}^2)\,dudv \tag{25}$$

$$F3(\lambda_1,\dots,\lambda_{m-1}) = \sum_{i,k}\iint_A (\mathbf{r}_{uuu}^2 + \mathbf{r}_{uu}^2 + 2\mathbf{r}_{uv}^2 + \mathbf{r}_{vv}^2)\,dudv, \tag{26}$$

$$A = [0,1]\times[0,1],$$

where the integrals have to be summed up for the patches $\mathbf{r}_{ik}(u,v)$ $(i = 1,2;\ k = 1,\dots,m-1)$ forming the closing part. Other fairness functionals approximating the thin plate energy for parametric surfaces are given in [3] and [4].

Using the quadratic approximation of a thin plate energy function and the assumption $g_{12} = 0$ are widely spread in practice and in publications, when the surface is nearly isometrically parametrized. In our case, the surface parametrization is far from being isometric, due to the presence of a singular point. Nevertheless, as demonstrated by the examples, the fairness functionals still produce reasonable smooth surfaces, avoiding wiggles and oscillations. Valid approximations for the fairness criteria in the neighbourhood of a singular point could be derived using Greiner's data-dependent functionals [3].

The fairing process means that the minimum location of one of these functions has to be found. The fairness functionals are quadratic expressions of control points computed from the boundary conditions at the closing point in (18)–(23). Consequently, the fairness functionals are quadratic in the variables λ_k $(k = 1,\dots,m-1)$, where $\lambda_m = \lambda_1$ due to the closed cross-sectional v parameter lines. The vector magnitudes λ_k are therefore solutions of the equations

$$\frac{\partial F}{\partial \lambda_k} = 0, \quad k = 1, \ldots, m-1,$$

where F denotes one of the functions $F1$, $F2$ and $F3$. According to this, the fairing problem leads to a system of linear equations of the size $m-1$ (20 and 12 in the examples).

The surface shown in Fig. 11 is generated by minimizing the fairness functional $F2$. The expression has been computed by symbolic integration which yields 111 terms for a B-spline patch of bidegree (3,2). The computed tangent magnitudes are between 11 and 16. The closing point P is the same as in the solutions in Figs. 8 and 9.

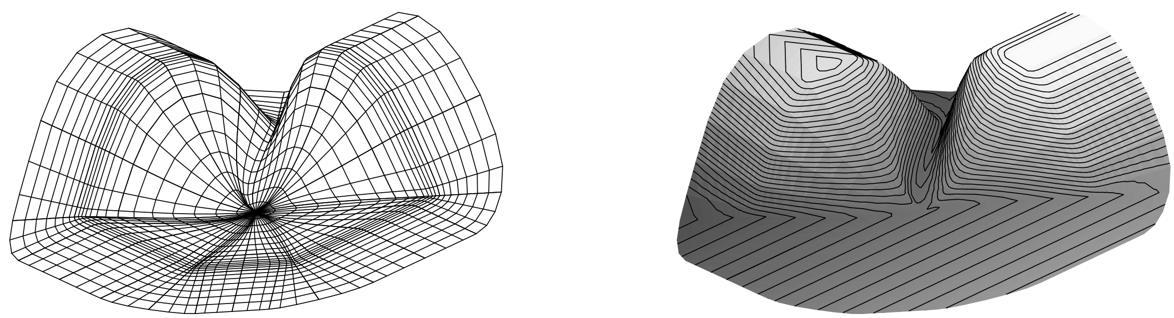

Figure 11: Closing part with faired tangent magnitudes

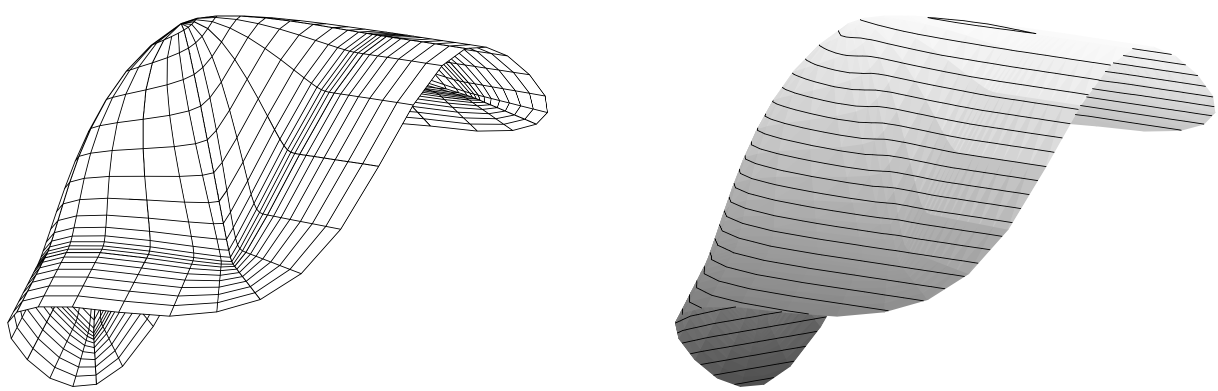

Figure 12: Closing part computed with the extended fairness functional

Our next goal is to optimize the position of the closing point P. An obvious idea is to consider its coordinates (x, y, z) as variables of the fairness functional, and to minimize it for $\lambda_1, \ldots, \lambda_{m-1}, x, y, z$. The results of the tested examples have shown that in this way the shape of the closing part has become too flat, even slightly concave, which is far from the desired solution, especially in the case of a suitcase corner.

Our proposition for the fairing process is to add a term to the fairness functional F which is the squared distance of the variable closing point $P(x, y, z)$ and its user input denoted by $P_0(x_0, y_0, z_0)$. Consequently, the minimum location of the extended functional

$$F + (x - x_0)^2 + (y - y_0)^2 + (z - z_0)^2$$

has to be computed for the variables $\lambda_1, \ldots, \lambda_{m-1}, x, y, z$, where F is one of the fairing functionals $F1$, $F2$ or $F3$ expressed with the user specified initial position P_0 of the closing point.

The surface in Fig. 12 is generated by minimizing the extended fairness functional $F2$ with the squared distance, where the initial point P_0 is the same as in the earlier example. The filling part shows a well-shaped form with a closing point by approx. 2 units inwards from the initial point.

Several examples have been computed also with the functionals $F1$ and $F3$. The closing surfaces that are least wavy have been generated with the extended functional $F2$.

6. Curvature conditions

The closing point is a singular point in the given parametric representation, where the surface normal does not exist. Consequently, the normal curvatures and Gauss curvature do not exist at this point either. However, the u parameter lines in the "radial" directions end with prescribed tangent vectors lying in a prescribed tangent plane (in the geometric sense) whose normal vector is $\mathbf{N}$. In such cases the Gauss curvature can be estimated by a method based on the curvature computation of the surface lines in normal sections ([16]). The converse problem is whether curvature values can be prescribed at the closing point.

A solution of this problem can be given by resmoothing the closing surface under prescribed normal curvature values of the patches $\mathbf{r}_{1k}(u, v)$ in the directions $(\dot{u}, \dot{v}) = (1, 0)$ at $(u, v) = (0, 0)$ $(k = 1, \ldots, m - 1)$ as follows. The formula of the normal curvature in this special direction leads to

$$\langle \frac{\partial^2}{\partial u^2} \mathbf{r}_{1k}(0, 0), \mathbf{N} \rangle / \lambda_k^2,$$

where $<, >$ denotes scalar product, λ_k is the magnitude of the tangent $\frac{\partial}{\partial u}\mathbf{r}_{1k}(0, 0)$ and $\mathbf{N}$ is the surface normal substituted by the prescribed unit normal vector. According to the requirement, this normal curvature has a user specified value κ_0 at the point $(u, v) = (0, 0)$. The fairing problem now will be formulated as a conditional extremum problem, minimizing one of the fairness functionals F under the condition

$$COND = \kappa_0 \lambda_k^2 - \langle \frac{\partial^2}{\partial u^2} \mathbf{r}_{1k}(0, 0), \mathbf{N} \rangle = 0.$$

In the special case of uniform parametrization

$$\frac{\partial^2}{\partial u^2} \mathbf{r}_{1k}(0, 0) = (V_{11}^{(k)} - 2V_{21}^{(k)} + V_{31}^{(k)} + V_{12}^{(k)} - 2V_{22}^{(k)} + V_{32}^{(k)})/2$$

Considering $V_{31}^{(k)}$ and $V_{32}^{(k)}$ fixed and equations (18)–(23) the variables are λ_k and λ_{k+2}. The Lagrange method looks for the extremum of the objective function

$$F + \mu\, COND,$$

where the Lagrange multiplier μ is an additional variable. The derivatives are now nonlinear functions of the variables, therefore the solution method has to be simplified in the following way. The fairness function is computed for the patches $\mathbf{r}_{1k}(u, v)$ and $\mathbf{r}_{2k}(u, v)$ $(k = 1, \dots, m-1)$, and the minimization process will be carried out successively while going around the center point. The objective function has the variables λ_k, λ_{k+2} and μ_k, and a system of nonlinear equations has to be solved in each step. The systems of equations are disjunct in their unknowns if κ_0 is prescribed for each second radial patch boundary (i.e. for each second k value). The net of control vertices (18)–(23) belonging to the actual solution slides around the center point accordingly.

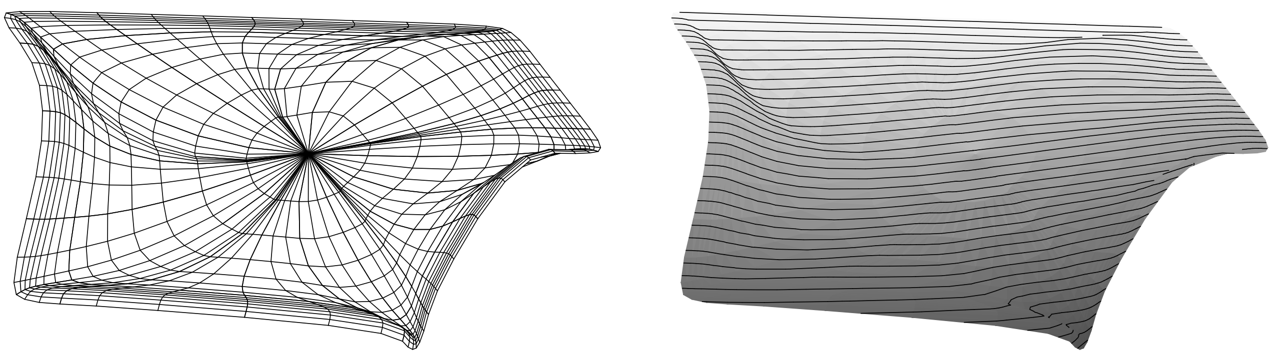

Figure 13: House corner with user specified tangent magnitudes

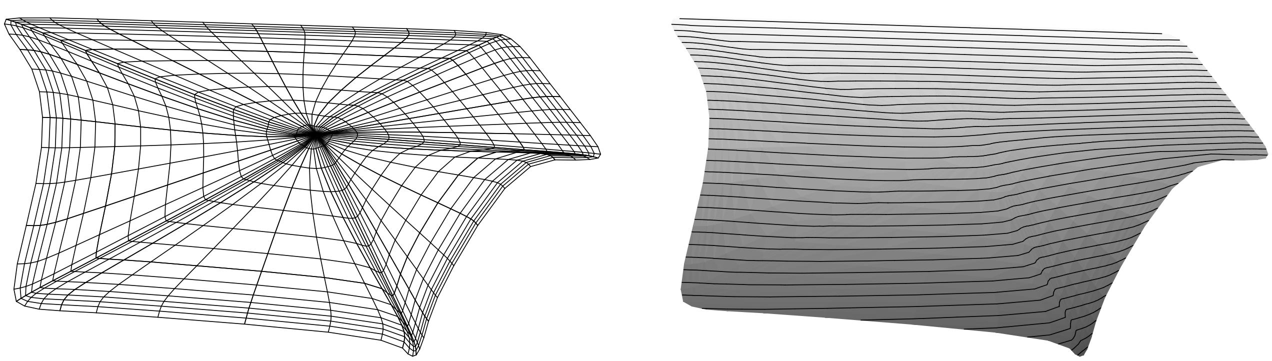

Figure 14: Resmoothed house corner

The surface filling a "house corner" pentagonal hole in Fig. 13 has been resmoothed by the fairness functional $F2$ with $\kappa_0 \in [-0.5, 0.5]$ and shown in Fig. 14. This surface satisfies similar boundary conditions as the blending surface in [12], but there with user specified tangent magnitudes, and here with tangent magnitudes determined by the fairing method above.

Conclusions

A method has been presented for filling an n-sided hole bounded by arbitrary differentiable surfaces. It produces a B-spline surface of degree $(3, 2)$ that matches the boundary curve segments of the hole and prescribed tangent vector fields (e.g. cross derivatives) along them with contact of second order. In this way the surface filling the hole joins with G^1 continuity to the surrounding surfaces. The algorithm works on the B-spline representation and uses fairing functionals for the computation of tangent magnitudes and for the adjustment of the central point of the hole. Further, a method has been given for resmoothing the generated B-spline surface according to prescribed normal curvatures at the closing point.

The computations and the majority of figures have been made by MATHEMATICA ([17]), the surfaces with level curves and ZGRAYSCALE shading by Maple 7.

References

[1] B.K. Choi, W.S. Yoo, C.S. Lee: *Matrix representation for NURB curves and surfaces*. Computer-Aided Design **22**, 235–239 (1990).

[2] H. Grabowski, X. Li: *Coefficient formula and matrix of nonuniform B-spline functions*. Computer-Aided Design **24**, 637–642 (1992).

[3] G. Greiner: *Variational design and fairing of spline surfaces*. Computer Graphics Forum **13**, no. 3, 143–154 (1994).

[4] H. Hagen, G. Schulze: *Automatic smoothing with geometric surface patches*. Computer Aided Geometric Design **4**, 231–235 (1987).

[5] J. Hoschek, D. Lasser: *Grundlagen der geometrischen Datenverarbeitung*. 2nd ed., B.G. Teubner, Stuttgart 1992.

[6] L.A. Piegl, W. Tiller: *Filling n-sided regions with NURBS patches*. Visual Computer **15**, 77–89 (1999).

[7] H. Prautzsch: *Freeform splines*. Computer Aided Geometric Design **14**, 201–297 (1997).

[8] H. Qin, D. Terzopoulos: *D-Nurbs: A Physics-based framework for geometric design*. IEEE Transactions on Visualisation and Computer Graphics **2**, no. 1, 85–96 (1996).

[9] U. Reif: *A refinable space of smooth spline surfaces of arbitrary topological genus*. Journal of Approximation Theory **90**, 174–199 (1997).

[10] G. Renner: *A method of shape description for mechanical engineering practice*. Comput. Ind.} **3**, 137–142 (1982).

[11] D.F. Rogers, J.A. Adams: *Mathematical Elements for Computer Graphics*. 2nd ed., McGraw-Hill Inc., 1990.

[12] M. Schichtel: *G^2 blend surfaces and filling of n-sided holes*. IEEE Computer Graphics and Applications **13**, 68–73 (1993).

[13] M. Szilvási-Nagy: *Shaping and fairing of tubular B-spline surfaces*. Computer Aided Geometric Design **14**, 699–706 (1997).

[14] M. Szilvási-Nagy: *Closing pipes by extension of B-spline surfaces*. KoG, Information Journal of Croatian Society for Constructive Geometry and Computer Graphics **3**, 13–19 (1998).

[15] M. Szilvási-Nagy: *Almost curvature continuous fitting of B-spline surfaces.* J. Geometry Graphics **2**, 33–43 (1998).

[16] F.C. Wolter, S.T. Tuohy: *Curvature computations for degenerate surface patches.* Computer Aided Geometric Design **9**, 241–270 (1992).

[17] S. Wolfram: *Mathematica: A System for Doing Mathematics by Computer.* Addison-Wesley Publishing Company, 1991.

Received May 30, 2001; final form June 26, 2002